Supporting Information

Pannasch et al. 10.1073/pnas.1016650108

SI Methods

Antibodies. The following primary antibodies were used: NeuN mouse monoclonal antibody and Vimentin goat polyclonal antibody (Chemicon); PSD-95 mouse monoclonal antibody (BD Transduction Labs); Synaptophysin rabbit polyclonal antibody (Dakocytomation); S-100 rabbit polyclonal antibody, GFAP rabbit polyclonal antibody, and Tubulin mouse monoclonal antibody (Sigma); EAAT3 (EAAC1) mouse monoclonal antibody (Millipore); EAAT4 rabbit polyclonal antibody (Santa Cruz); and GAPDH mouse monoclonal antibody (Sigma). The following HRP-conjugated secondary antibodies were used: donkey anti rabbit IgG (Amersham Biosciences), goat anti-guinea pig IgG (Gene Tex), and goat anti-mouse IgG (Santa Cruz). The following fluorescent dye-conjugated secondary antibodies were used in appropriate combinations: goat anti-mouse, goat anti-rabbit, or rabbit anti-goat IgG Alexa 488 or 555 conjugated antibodies (Molecular Probes).

Immunoblotting. Hippocampi from wild-type and $Cx30^{-/-}Cx43^{-/-}$ mice were frozen, pulverized, and homogenized in 2% SDS with protease inhibitor mixture, β-glycerophosphate (10 mM), and orthovanadate (1 mM). Equal amounts of protein were separated on a 10% PAGE gel followed by transfer to nitrocellulose membranes. Proteins were detected by immunoblotting using the HRP-ECL kit from Perkin-Elmer. Tubulin or GAPDH was used as a loading control.

Immunohistochemistry. Mice were anesthetized and perfused with PBS and their brains rapidly removed and frozen in isopentane cooled at −30 °C. Coronal sections (20 μm) were cut on a cryostat, collected on slides, and fixed with 4% paraformaldehyde in PBS for 30 min at 4 °C. Coronal sections or fixed hippocampal slices were permeabilized and immunoblocked with PBS, containing 0.2% gelatin and 0.2% Triton-X100, for 1 h and processed for immunostaining by overnight incubation at 4 °C with primary antibodies diluted in PBS. After three washes, sections were incubated for 2 h at room temperature with appropriate secondary antibodies. Biocytin revelation was performed by incubating slices in TRITC-conjugated streptavidin (Molecular Probes). After several washes, slices were mounted in Fluoromount (Southern Biotechnology) and examined with a confocal laser-scanning microscope (Leica TBCS SP2, SP5), equipped with 16×, 40×, and 63× objectives. Stacks of consecutive confocal images taken at 0.5-μm intervals were acquired sequentially with two lasers (argon, 488 nm; helium/neon, 543 nm) and Z projections were reconstructed using Leica confocal software. Cell counting was performed with ImageJ software. NeuN-positive cells were counted in a CA1 pyramidal cell layer in randomly selected fields (540 × 430-μm length/width, one optical plane), whereas S100-positive cells were counted in *stratum radiatum*, in randomly selected fields of image stacks (400 × 400 × 20 μm, length/width/depth). Domain areas of astrocytes were defined by surrounding their process endings labeled with GFAP. To measure astrocytic process length, double staining of GFAP, an astrocyte-specific cytoskeleton marker, and Topro, a nucleus marker, was performed in hippocampal slices. The distance between the middle of the nucleus and the longest process of *stratum radiatum* astrocytes was measured with ImageJ.

Sulforhodamine 101 Labeling. Sulforhodamine 101 (SR101) labeling of astrocytes was achieved by incubating hippocampal slices in artificial cerebrospinal fluid (ACSF) containing 1 μM SR101 for 30 min at 30 °C, as previously decribed (1). Images were taken on acute slices using a confocal laser-scanning microscope (Leica TBCS SP2), equipped with a 63× objective. Stacks of consecutive confocal images taken at 0.5-μm intervals were acquired sequentially with a laser (helium/neon, 543 nm) and Z projections were reconstructed using ImageJ.

Electrophysiology. Acute transverse hippocampal slices (300–400 μm) were prepared as previously described (2) from 16- to 25-d-old wild-type and $Cx30^{-/-}Cx43^{-/-}$ mice. Slices were maintained at room temperature in a storage chamber containing ACSF (containing 119 mM NaCl, 2.5 mM KCl, 2.5 mM $CaCl_2$, 1.3 mM $MgSO_4$, 1 mM NaH_2PO_4, 26.2 mM $NaHCO_3$, and 11 mM glucose, saturated with 95% O_2 and 5% CO_2) for at least 1 h before recording. Slices were transferred to a submerged recording chamber mounted on an Olympus BX51WI microscope equipped for infrared-differential interference (IR-DIC) microscopy and were perfused with ACSF at a rate of 1.5 mL/min at room temperature. All experiments were performed in the presence of picrotoxin (100 μM) and a cut was made between CA1 and CA3 to prevent the propagation of epileptiform activity, except for recordings of IPSCs. Extracellular field and whole-cell patch-clamp recordings were performed. Evoked postsynaptic or astrocytic responses were induced by stimulating Schaffer collaterals (0.1 Hz) in CA1 *stratum radiatum* with ACSF-filled glass pipettes. *Stratum radiatum* astrocytes were identified by their small cell bodies, low input resistance (~20 MΩ), high resting potentials (~ −80 mV), and linear IV curves. Field excitatory postsynaptic potentials (fEPSPs) were recorded from 400-μm slices with glass pipettes (2–5 MΩ) filled with ACSF and placed in *stratum radiatum*. Stimulus artifacts were blanked in sample traces. Somatic whole-cell recordings were obtained from visually identified CA1 pyramidal cells and *stratum radiatum* astrocytes, using 5- to 10-MΩ glass pipettes filled with 105 mM K-gluconate, 30 mM KCl, 10 mM Hepes, 10 mM phosphocreatine, 4 mM ATP-Mg, 0.3 mM GTP-Tris, and 0.3 mM EGTA (pH 7.4, 280 mOsm); or, for synaptic activity recordings, 115 mM $CsMeSO_3$, 20 mM CsCl, 10 mM Hepes, 2.5 mM $MgCl_2$, 4 mM Na_2ATP, 0.4 mM NaGTP, 10 mM Na-phosphocreatine, 0.6 mM EGTA, 0.1 mM spermine, and 5 mM QX314 (pH 7.2, 280 mOsm); or, for recording of EPSCs at −60 mV and IPSCs at 0 mV, 107.5 mM Csgluconate, 20 mM Hepes, 0.2 mM EGTA, 8 mM Na-gluconate, 8 mM TEA-Cl, 4 mM Mg-ATP, 0.3 mM Na_3-GTP, and 5 mM QX314 (pH 7.2, 280 mOsm). Astroglial whole-cell glutamate transporter currents and potassium currents were evoked by stimulation of Schaffer collaterals and were recorded simultaneously with fEPSPs. The field recording pipette was placed 50 μm away from the recorded astrocyte and transporter currents were blocked by DL-threo-β-Benzyloxyaspartatic acid (TBOA, 200 μM), while potassium currents were blocked by kynurenic acid (5 mM). To isolate the GLT current, the current trace in the presence of kynurenic acid and TBOA was subtracted from the current in the presence of kynurenic acid (Fig. S5 *B* and *C*). Astrocytic potassium currents were isolated by subtraction of the current in the presence of kynurenic acid from the total current (control, Fig. S5 *E* and *F*). For intercellular dye-coupling experiments, the internal solution contained sulforhodamine B (1 mg/mL), which diffused passively in astrocytes patched in current-clamp mode during 20 min. For AMPA/NMDA ratios, evoked AMPAR-mediated EPSCs were measured at −70 mV, and NMDAR-mediated EPSCs were measured at +40 mV and at a latency of 60 ms, when the AMPAR EPSC had fully decayed. Paired-pulse facilitation was performed by delivery of two stimuli at an interval of 40 ms. For minimal stimulation experiments, data were collected and analyzed as described previously (3). Minimal

stimulation was achieved by evoking a CA1 pyramidal neuron EPSC response by Schaffer collateral stimulation and stimulation intensity was adjusted to putatively stimulate a single or very few synapses. To estimate the failure rate, the number of responses with an amplitude less than three times the SD of the noise was determined and expressed as a percentage of the total number of stimulations. Traces including spontaneous EPSCs temporally uncorrelated with the stimulus were not included in the analysis. The enhanced release probability in $Cx30^{-/-}Cx43^{-/-}$ mice was lowered to the wild-type level by reducing extracellular $CaCl_2$ to 2.2 mM. To keep extracellular divalent ion concentration constant, $MgSO_4$ was increased to 1.6 mM. The noise amplitude was calculated on traces after inhibition of AMPA responses by CNQX. The corresponding NMDA current was measured at +40 mV. To estimate the failure rate, the number of responses with amplitudes bigger than the calculated noise was determined and expressed as percentage of the total number of stimulations.

LTP was induced by tetanic stimulation of Schaffer collaterals (two trains of 100 Hz for 1 s, 20 s apart). LTD was induced by 1-Hz stimulation of Schaffer collaterals over 15 min. AMPA-mediated whole-cell currents were obtained by local application of 10 μM (S)-a-Amino-3-hydroxy-5-methyl-4-isoxazolepropionic acid (S-AMPA) for 5 s in the presence of 100 μM cyclothiazide and 0.5 μM TTX, using a large barrel (250 μm diameter) targeting the soma, as well as most of the dendritic tree of the recorded neuron. Synaptically evoked NMDAR EPSCs were recorded in the presence of 10 μM CNQX at +50 mV or −70 mV to inhibit or not, respectively, postsynaptic neuronal GLTs as previously described (4). When recordings were performed at −70 mV, slices were stored and recorded in ACSF where $MgSO_4$ was replaced by $CaCl_2$, and 1 mM kynurenic acid was added to reduce excitotoxicity during slice storage. Internal solution with Cs was prepared as previously described (4).

Recordings were acquired with Axopatch-1D amplifiers (Molecular Devices), digitized at 10 kHz, filtered at 2 kHz, and stored and analyzed on a computer using Pclamp9 and Clampfit9 software (Molecular Devices). All data are expressed as mean ± SEM. Statistical significance for comparisons was determined by unpaired or paired *t* tests. Picrotoxin, D-aspartate, and D-AA were obtained from Sigma and all other chemicals were from Tocris.

Deconvolution Analysis to Derive Glutamate Clearance Time Course from GLT Currents. The glutamate clearance time course was obtained by a deconvolution procedure of the astroglial GLT current, as previously described (5). The total astroglial recorded current $I(t)$ is the sum of the GLT current $I_{GLT}(t)$ and a slowly decaying residual current $I_{res}(t)$, such that $I(t) = I_{GLT}(t) + I_{res}(t)$. To extract the GLT and residual components from the total current, we used the analytical expression

$$I(t) = I_{GLT}(t) + I_{res}(t) = a_{GLT}(1 - e^{-\lambda t})e^{-\mu t} + a_{res}(1 - e^{-\nu t})$$

to fit the recorded total astroglial current. Whereas the amplitudes a_{GLT} and a_{res} of the GLT and residual currents and the rising λ and decay μ rates were obtained as outputs of the fitting procedure, the residual rising rate ν was an input parameter, which was estimated from the measured residual current rising times in the presence of 200 μM TBOA to block GLTs. The measured residual current rising times were $\nu^{-1} = 4.6 \pm 0.6$ ms for wild-type mice ($n = 5$) and 4.9 ± 0.7 ms for $Cx30^{-/-}Cx43^{-/-}$ mice ($n = 5$).

The GLT current can be described as a convolution of a filter $f(t)$ with the clearance $cl(t)$, given by the formula $I_{GLT}(t) = \int_0^t f(u)cl(t-u)du$. The filter $f(t)$ was derived from recordings where the GLT decay was prolonged and dominated by the slow time course of glutamate clearance due to a partial block of GLTs by 20 μM TBOA (6, 7). In that case, the glutamate clearance was approximated by $cl_{tboa}(t) = e^{-\mu t}$, and by deconvolution of this clearance from the GLT current inline-formula$>I_{GLT}(t) = a_{GLT}(1 - e^{-\lambda t})e^{-\mu t}$ (*), we obtain the filter $f(t) = a_{GLT}\lambda e^{-(\lambda+\mu)t} \approx a_{GLT}\lambda e^{-\lambda t}$, where in the last expression we used the approximation $\lambda >> \mu$ (the decay time of the current is large compared with its rising time). At this stage, all of the parameters of the filter formula are known. We then computed the mean filter for wild-type and $Cx30^{-/-}Cx43^{-/-}$ mice, by averaging the filters from different cells of each genotype, with the filter amplitudes rescaled to 1: $f_{mean}(t) = (1/n)\sum_{k=1}^{n} e^{-\lambda_k t}$, where λ_k is the rising rate of cell k.

To obtain the glutamate clearance time course for wild-type and $Cx30^{-/-}Cx43^{-/-}$ mice in control conditions, with uptake fully intact, we deconvolved (using the deconvolution numerical procedure from Matlab) these mean filters from the extracted GLT current [see equation (*) in previous paragraph] obtained from the recorded total current in individual cells in control conditions. To extract the glutamate clearance time, we fitted the initial phase of the glutamate clearance time course by a single exponential function. By averaging over the cell population, we obtained the mean glutamate clearance time course (Fig. 4*C*, *Upper*) and time (Fig. 4*C*, *Lower*) for wild-type and $Cx30^{-/-}Cx43^{-/-}$ mice.

Extracellular Volume Measurements. The relative changes in the extracellular volume in the CA1 region during Schaffer collateral stimulation were determined by measuring the time-dependent concentration changes of an extracellular marker, tetramethylammonium (TMA), to which cell membranes are relatively impermeable (Fig. 6*A*). Changes in the extracellular concentration of TMA ions ($[TMA^+]_e$), which are inversely proportional to ECS volume, were detected using double-barreled ion-selective microelectrodes (TMA^+-ISMs), prepared as previously described (8). In brief, the tip of the ion-selective channel contained the liquid ion exchanger (Corning 477317; currently available as IE 190 from WPI), and the channel was backfilled with 100 mM TMACl (Sigma), whereas the reference barrel contained 150 mM NaCl. The TMA^+-ISMs were calibrated in solutions containing 0.1, 0.5, 1, 5, and 10 mM TMACl with a background of 150 mM NaCl and 3 mM KCl. For measurements of the TMA^+ baseline, slices were perfused continuously with ACSF containing 1 mM TMACl. The relative changes in the extracellular volume were extracted from the changes in the TMA^+ baseline concentration using the following equation (9):

$$\Delta\,\text{volume}(\%) = \left(1 - \left[TMA^+\right]_e \text{before stimulation} / \left[TMA^+\right]_e \text{during stimulation}\right) \times 100.$$

1. Nimmerjahn A, Kirchhoff F, Kerr JN, Helmchen F (2004) Sulforhodamine 101 as a specific marker of astroglia in the neocortex in vivo. *Nat Methods* 1:31–37.
2. Rouach N, et al. (2005) TARP gamma-8 controls hippocampal AMPA receptor number, distribution and synaptic plasticity. *Nat Neurosci* 8:1525–1533.
3. Isaac JT, Nicoll RA, Malenka RC (1995) Evidence for silent synapses: Implications for the expression of LTP. *Neuron* 15:427–434.
4. Diamond JS (2001) Neuronal glutamate transporters limit activation of NMDA receptors by neurotransmitter spillover on CA1 pyramidal cells. *J Neurosci* 21:8328–8338.
5. Diamond JS (2005) Deriving the glutamate clearance time course from transporter currents in CA1 hippocampal astrocytes: Transmitter uptake gets faster during development. *J Neurosci* 25:2906–2916.
6. Bergles DE, Jahr CE (1997) Synaptic activation of glutamate transporters in hippocampal astrocytes. *Neuron* 19:1297–1308.
7. Diamond JS, Jahr CE (2000) Synaptically released glutamate does not overwhelm transporters on hippocampal astrocytes during high-frequency stimulation. *J Neurophysiol* 83:2835–2843.
8. Sykova E (1992) Ionic and volume changes in the microenviroment of nerve and receptor cells. *Progress in Sensory Physiology*, ed Ottoson D (Springer, Berlin), Vol 13, pp 1–176.
9. Svoboda J, Syková E (1991) Extracellular space volume changes in the rat spinal cord produced by nerve stimulation and peripheral injury. *Brain Res* 560:216–224.

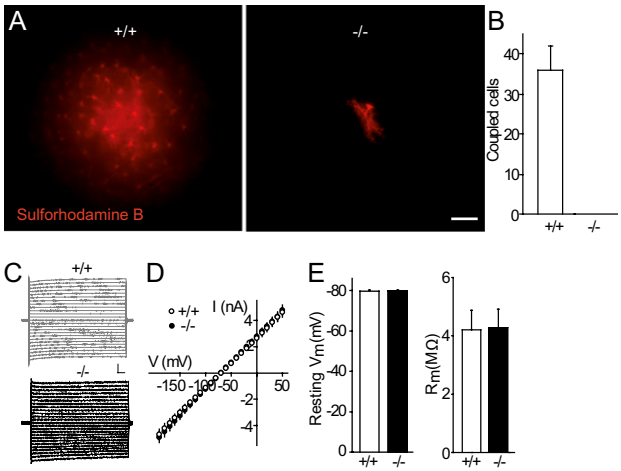

Fig. S1. Unchanged intrinsic membrane properties of uncoupled Cx30$^{-/-}$Cx43$^{-/-}$ astrocytes. (*A*) Astrocytes deficient for Cx43 and Cx30 ($^{-/-}$) are uncoupled, as shown by sulforhodamine B injections, whereas wild-type astrocytes ($^{+/+}$) show dye coupling. (Scale bar, 50 μm.) (*B*) Quantification of sulforhodamine B-coupled cells (Cx30$^{-/-}$Cx43$^{-/-}$, n = 18, WT, n = 21). (*C*) Whole-cell current profiles from CA1 astrocytes evoked by 150 ms voltage steps (−200–+40 mV). (Scale bar, 1 nA, 10 ms.) (*D* and *E*) No difference was found in current–voltage (I/V) plots (*D*) and resting membrane potential (V_m) and membrane resistance (R_m) (*E*) in astrocytes from Cx30$^{-/-}$Cx43$^{-/-}$ mice (n = 28), compared with cells from wild-type mice (n = 25).

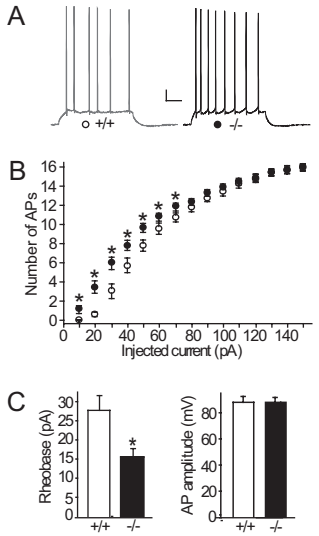

Fig. S2. Enhanced excitability in CA1 pyramidal cells from Cx30$^{-/-}$Cx43$^{-/-}$ mice. (*A*) Representative traces of CA1 pyramidal cell firing pattern from wild-type and Cx30$^{-/-}$Cx43$^{-/-}$ mice during depolarization by 40-pA injection for 500 ms. Cells were held at −60 mV by adjusting the holding current. (Scale bar, 10 mV, 100 ms.) (*B* and *C*) Enhanced action potential (AP) firing in pyramidal cells from Cx30$^{-/-}$Cx43$^{-/-}$ mice (n = 22) compared with wild type (P < 0.05, n = 18, *B*), resulting from a lower rheobase (P < 0.01, *C*). (*C*) Unchanged AP amplitude in pyramidal cells from Cx30$^{-/-}$Cx43$^{-/-}$ mice.

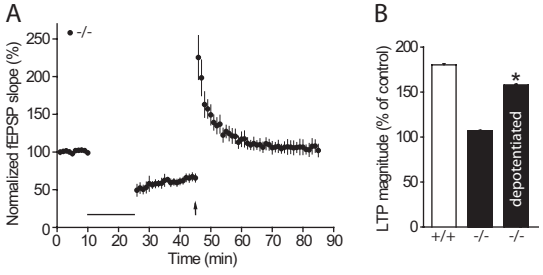

Fig. S3. Synapse depotentiation restores LTP in Cx30$^{-/-}$Cx43$^{-/-}$ mice.(*A*) LTD induction (1 Hz stimulation, 15 min, solid line) before tetanic stimulation of Schaffer collaterals (two trains of 100 Hz for 1 s, 20 s apart, arrow) restored LTP in Cx30$^{-/-}$Cx43$^{-/-}$ mice, as quantified in the bar graph (*B*) (normalized LTP magnitude measured 30–40 min after LTP induction, P < 0.001, depotentiated Cx30$^{-/-}$Cx43$^{-/-}$ slices, n = 5; Cx30$^{-/-}$Cx43$^{-/-}$ slices, n = 9; wild-type slices, n = 9).

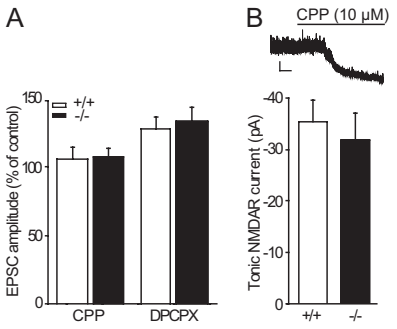

Fig. S4. Levels of gliotransmitter release during basal evoked neuronal activity and ambient glutamate are unchanged in $Cx30^{-/-}Cx43^{-/-}$ mice. (*A*) Gliotransmitter release (glutamate, D-serine, ATP) evoked by single stimulation of the Schaffer collaterals in $Cx30^{-/-}Cx43^{-/-}$ hippocampi (CPP, $n = 5$; DPCPX, $n = 9$) is comparable to wild-type slices (CPP, $n = 5$; DPCPX, $n = 9$). (*B*) Ambient glutamate levels, in the absence of stimulation, are comparable in $Cx30^{-/-}Cx43^{-/-}$ ($n = 7$) and wild-type hippocampal slices ($n = 8$), as revealed by holding current recordings in CA1 pyramidal cells held at +40 mV before and after application of the NMDAR antagonist CPP (10 μM). A representative current trace is shown above the bar graph. (Scale bar, 10 pA, 1 min.)

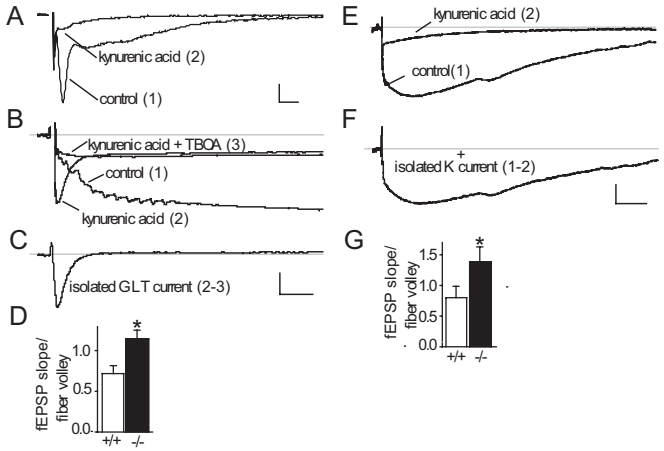

Fig. S5. Pharmacological isolation of astroglial potassium and glutamate transporter currents evoked by Schaffer collateral stimulation. (*A* and *B*) Simultaneous recordings of the field potential (*A*, 1) and astroglial whole-cell current in response to a single Schaffer collateral stimulation are shown (*B*, 1). (Scale bars: 0.2 mV, 5 ms; and 5 pA, 50 ms.) Application of kynurenic acid (5 mM) inhibits the postsynaptic response (fEPSP; *A*, 2) and reduces the astrocytic potassium current component, unmasking the GLT current (*B*, 2). In the presence of kynurenic acid and TBOA (200 μM), an inhibitor of GLTs, a slow current component is remaining (*B*, 3). (*C*) Subtraction of this remaining current (*B*, 2 and 3), isolates the GLT current. (*D*) The corresponding neuronal transmission was calculated by the fEPSP slope/fiber volley ratio ($P < 0.05$, $Cx30^{-/-}Cx43^{-/-}$, $n = 6$; WT, $n = 6$). (*E* and *F*) Isolation of the evoked long-lasting potassium (K^+) current component in astrocytes is illustrated. Application of kynurenic acid inhibits the postsynaptic response (fEPSP; *A*, 2) and reduces the astroglial current to the GLT and a slow current component (*E*, 2). Subtraction of these remaining currents (*E*, 1 and 2) isolates the K^+ current component evoked by neuronal activity (*F*). (Scale bar, 5 pA, 1 s.) (*G*) The associated excitatory synaptic transmission (fEPSP slope/fiber volley ratio) ($P < 0.05$, $Cx30^{-/-}Cx43^{-/-}$, $n = 8$; WT, $n = 7$).

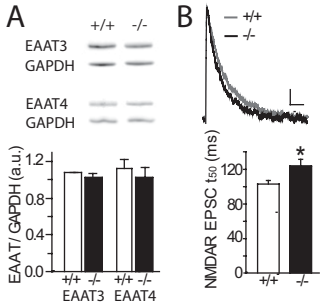

Fig. S6. Neuronal glutamate transporter levels and contribution to increased extracellular glutamate in $Cx30^{-/-}Cx43^{-/-}$ mice. (*A*) Similar levels of the neuronal GLTs EAAT3 and EAAT4 in $Cx30^{-/-}Cx43^{-/-}$ ($n = 3$) and wild-type hippocampi ($n = 3$) are shown, as analyzed by Western blot quantification. GAPDH was used as loading control. a.u., arbitrary units. (*B*) Inhibition of neuronal GLTs in the postsynaptic neuron by depolarization at +50 mV does not abolish the increased glutamate levels in $Cx30^{-/-}Cx43^{-/-}$ mice ($n = 7$), compared with wild-type mice ($P < 0.05$, $n = 6$), as assessed by the prolonged decay kinetics (t_{50}) of evoked NMDAR EPSCs (recorded at +50 mV in 10 μM CNQX). (Scale bar, 20 pA, 150 ms.)